

See discussions, stats, and author profiles for this publication at: <https://www.researchgate.net/publication/258341606>

# XPS, UV-Vis, FTIR, and EXAFS studies to investigate the binding mechanism of N719 dye onto oxalic acid treated TiO<sub>2</sub> and its implication on photovoltaic properties

ARTICLE in THE JOURNAL OF PHYSICAL CHEMISTRY C · OCTOBER 2013

Impact Factor: 4.77 · DOI: 10.1021/jp4062994

---

CITATIONS

6

---

READS

123

10 AUTHORS, INCLUDING:



Vibha Saxena

Bhabha Atomic Research Centre

53 PUBLICATIONS 658 CITATIONS

SEE PROFILE



Anil Kumar Chauhan

Bhabha Atomic Research Centre

43 PUBLICATIONS 194 CITATIONS

SEE PROFILE



Veerender Putta

Bhabha Atomic Research Centre

33 PUBLICATIONS 153 CITATIONS

SEE PROFILE



Shankar Koiry

Bhabha Atomic Research Centre

46 PUBLICATIONS 333 CITATIONS

SEE PROFILE

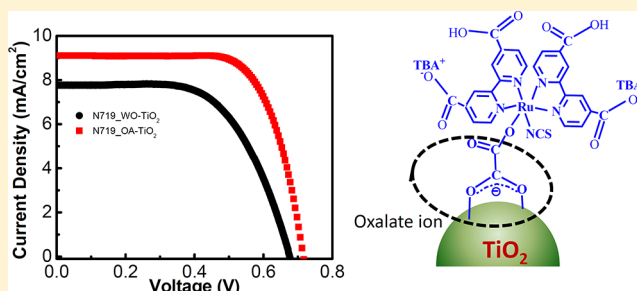
# XPS, UV–Vis, FTIR, and EXAFS Studies to Investigate the Binding Mechanism of N719 Dye onto Oxalic Acid Treated TiO<sub>2</sub> and Its Implication on Photovoltaic Properties

Jaspreet Singh,<sup>†</sup> Abhay Gusain,<sup>†</sup> Vibha Saxena,<sup>\*,†</sup> A.K. Chauhan,<sup>†</sup> P. Veerender,<sup>†</sup> S. P. Koiry,<sup>†</sup> P. Jha,<sup>†</sup> Avani Jain,<sup>‡</sup> D.K. Aswal,<sup>\*,†</sup> and S. K. Gupta<sup>†</sup>

<sup>†</sup>Technical Physics Division, Bhabha Atomic Research Centre, Trombay, Mumbai - 400085, Maharashtra, India

<sup>‡</sup>Centre for Converging Technologies, University of Rajasthan, Jaipur - 302004, Rajasthan, India

**ABSTRACT:** The anchoring mechanism of N719 dye molecules on oxalic acid treated TiO<sub>2</sub> (OA-TiO<sub>2</sub>) electrodes has been investigated using extended X-ray absorption fine structure (EXAFS) measurements, Fourier transform infrared spectroscopy (FTIR), UV–vis spectroscopy, and X-ray photoelectron spectroscopy (XPS). The FTIR spectroscopy of OA-TiO<sub>2</sub> electrodes revealed that the oxalic acid dissociates at the TiO<sub>2</sub> surface and binds through bidentate chelating and/or bidentate bridging. Analyses of EXAFS, FTIR, UV–vis, and XPS measurements of N719 dye loaded onto OA-TiO<sub>2</sub> revealed that the binding of N719 molecules takes place via interaction between the Ru atom of the dye and O<sup>−</sup> of bidentate bridged oxalate ions at the TiO<sub>2</sub> surface. This mechanism is quite different from the binding of N719 onto untreated TiO<sub>2</sub> (WO-TiO<sub>2</sub>) surface, where –COOH and SCN groups of the dye directly bind to the TiO<sub>2</sub> surface. The analyses of UV–vis data show that the amount of N719 dye loading onto OA-TiO<sub>2</sub> surface is much higher than that onto the native TiO<sub>2</sub> surface. In addition, the incident photon-to-current conversion efficiency (IPCE) measurements show that the presence of oxalate ions between the dye and TiO<sub>2</sub> surface favors efficient electron transfer and therefore improvement in device efficiency. The dye-sensitized solar cells fabricated using N719 dye sensitized onto OA-TiO<sub>2</sub> showed an efficiency of ~4.6%, which is significantly higher than that based on a WO-TiO<sub>2</sub> electrode (~3.2%).



## 1. INTRODUCTION

Dye-sensitized solar cells (DSSCs) are being investigated extensively as potential devices for harnessing solar power owing to ease of fabrication and their relatively low cost compared to conventional silicon solar cells.<sup>1–3</sup> Devices with efficiency exceeding 10% have been fabricated using nanoporous TiO<sub>2</sub> sensitized with Ru(II)-polypyridyl complexes, such as N3, N719.<sup>4</sup> It is well-established that modification of the TiO<sub>2</sub> surface plays a major role in determining the efficiency of the DSSCs. It has also been demonstrated that the short circuit current ( $J_{SC}$ ) and therefore the efficiency of the DSSC improves by the treatment of the TiO<sub>2</sub> electrode with 0.1 M HCl.<sup>5</sup> In addition, other acids such as HNO<sub>3</sub>, H<sub>3</sub>PO<sub>4</sub>, and H<sub>2</sub>SO<sub>4</sub> have also been reported to affect the photovoltaic properties and therefore the device efficiency.<sup>6–8</sup> The improvement in efficiency as a result of surface treatment in the DSSCs has been attributed to the negative movement of the TiO<sub>2</sub> conduction band edge (CBE), enhanced dye absorption, and reduced charge recombination. To understand the improvement in the device performance as a result of surface modifications, it is important to have knowledge about the interfacial properties of the materials involved in the fabrication of DSSCs. In general, at the TiO<sub>2</sub> semiconductor–dye interface, ultrafast electron injection from the excited dye to

the conduction band of the TiO<sub>2</sub> takes place, which is responsible for the improvement in the device efficiency. However, several recombination processes also occur at this interface that affect the overall device efficiency. Both injection and recombination dynamics are influenced by the electronic coupling between the dye and TiO<sub>2</sub> and thereby the binding mode of the dye to the TiO<sub>2</sub> surface. Therefore, the efficiency of the DSSCs, in addition to TiO<sub>2</sub> CBE movement, depends upon the interaction of the dye molecules with the TiO<sub>2</sub> surface.

In spite of the fact that the modified TiO<sub>2</sub> surface might lead to a change in the electron injection dynamics owing to a different binding mechanism of N719 dye molecules on the modified surface, this aspect has not been discussed in literature and there is no report yet describing the binding mechanism of the ruthenium complexes onto surface-modified TiO<sub>2</sub>. Nevertheless, the absorption orientation and electronic coupling of N719 on TiO<sub>2</sub> has been studied and discussed by several groups using vibrational spectroscopy, X-ray absorption spectroscopy, and computational model studies. Despite the

Received: June 26, 2013

Revised: September 6, 2013

Published: September 18, 2013

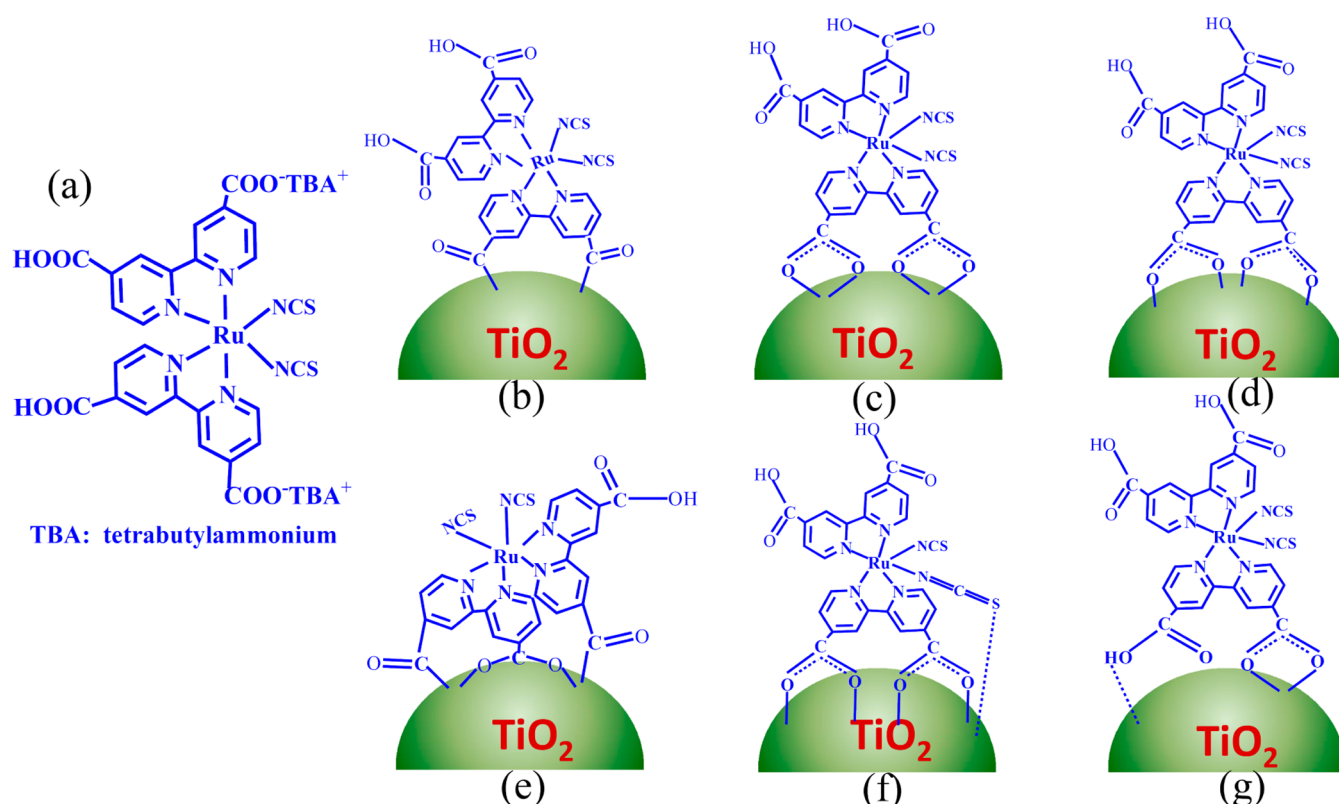


**Figure 1.** (a) N719 dye structure and Schematic presentations of binding of N719 dye on the TiO<sub>2</sub> surface: (b) ester linkage, (c) bidentate chelating, (d) bidentate bridging, (e) mixed bidentate and monodentate mode, (f) NCS group interacts with the TiO<sub>2</sub> surface, and (g) bidentate chelating and hydrogen bonding.

volume of work, the binding mechanism of N719 dye onto TiO<sub>2</sub> surface is not yet fully understood and remains a subject of debate. The various binding mechanisms proposed in the literature are summarized in Figure 1. The structure of N719 dye is shown in Figure 1a. As shown in Figure 1b, the first type of binding, known as ester type linkage, involves interaction of one or two oxygen atoms of the –COOH group with the Ti atoms of the TiO<sub>2</sub> surface, resulting in unidentate or bidentate co-ordination mode. Falaras et al. suggested this type of linkage based on a 20 cm<sup>−1</sup> shift in the carbonyl group observed in FTIR spectra.<sup>9</sup> The second type of binding involves the interaction of both oxygen atoms of COOH groups with either one or two Ti atoms, resulting in bidentate chelating or bridging, as depicted in Figure 1c and Figure 1d, respectively. This mechanism was proposed by Finnie et al., who studied the co-ordination of the dyes and of benzoic acid onto the TiO<sub>2</sub> surface.<sup>10</sup> On the basis of their results, they suggested that carboxylate attaches to the TiO<sub>2</sub> surface via bidentate chelating or bridging co-ordination using two carboxylic acid groups per dye molecule. Later, Nazeeruddin et al. investigated different ruthenium complexes to determine the specific carboxylic group (COO<sup>−</sup> or –COOH) involved in TiO<sub>2</sub> binding.<sup>11</sup> On the basis of FTIR analysis, they deduced that N719 dye absorbs on the TiO<sub>2</sub> surface in bridging mode via two carboxylic groups trans to the NCS group. Further, supporting data were provided by Leon et al. who carried out UV–vis, FTIR, and Raman measurements to investigate the absorption mechanism of N719 sensitizer on TiO<sub>2</sub>.<sup>12</sup> From the Raman measurements, the co-ordination of the N719 dye was proposed to occur through bridging or bidentate linkage. They confirmed their results by attenuated total reflectance FTIR (ATR-FTIR)

spectra, which provided a direct fingerprint of the deprotonation state of the carboxylic moieties. A third binding mechanism (Figure 1e) was also proposed on the basis of molecular dynamics simulations and electronic structure calculations. Accordingly, the N719 dye binding to the TiO<sub>2</sub> surface occurs through three carboxylic groups, one of which is attached to two Ti atoms in bidentate form while the other two are bound via monodentate mode.<sup>13</sup> In contrast to these findings, a fourth binding mechanism (Figure 1f), was also proposed in which the N719 dye molecules interact with the TiO<sub>2</sub> surface through the NCS group in addition to the bidentate bridging.<sup>14</sup> Recent studies by Lee et al. elucidated the role of Ti–OH/TiOH<sub>2</sub> groups in the binding mode of the dye.<sup>15</sup> On the basis of detailed vibrational spectroscopic studies of N719 dye absorbed on the TiO<sub>2</sub> surface, they proposed that the binding of the dye to TiO<sub>2</sub> occurs through two neighboring carboxylic acid/carboxylate groups via a combination of bidentate bridging and H-bonding involving a donating group from the N719 dye and acceptor from the Ti–OH group (Figure 1g).

Though most studies suggest anchoring of N719 dye on the TiO<sub>2</sub> surface via two carboxylate groups, the role of various kinds of surface treatments of the TiO<sub>2</sub> surface has not been reported to date. In our earlier work, we reported that the efficiency of the DSSC is improved significantly when a photoanode consisting of N3 dye loaded onto a formic acid treated TiO<sub>2</sub> surface or N719 dye loaded onto a carboxylic acid treated TiO<sub>2</sub> surface are utilized.<sup>16,17</sup> The analyses of the device characteristics in both cases revealed that the efficiency improvement occurred because of enhanced dye absorption onto the TiO<sub>2</sub> electrode and reduced recombination. This

resulted in an increase in both the  $J_{SC}$  and  $V_{OC}$  and therefore enhanced efficiency.

In this work, we report a detailed investigation of the binding mechanism of N719 dye onto the oxalic acid treated  $TiO_2$  surface using various characterization techniques, i.e., X-ray absorption fine structure (EXAFS) measurements, Fourier transform infrared spectroscopy (FTIR), UV-vis spectroscopy, and X-ray photoelectron spectroscopy (XPS). The results of these studies revealed that the binding of N719 molecules takes place via interaction between the Ru atom of the dye and  $O^-$  of bidentate bridged oxalate ions at  $TiO_2$  surface. This is in contrast to the binding of N719 onto untreated  $TiO_2$  surface, in which  $-COOH$  and  $SCN$  groups of the dye directly bind to  $TiO_2$  surface. The results of incident photon-to-current conversion efficiency (IPCE) measurements show that the presence of oxalate ions between the dye and  $TiO_2$  surface favors efficient electron transfer and therefore improves the device efficiency.

## 2. EXPERIMENTAL SECTION

**2.1. Fabrication of DSSC.** The photoelectrode was fabricated using the procedure reported earlier.<sup>17</sup> Briefly, a  $TiO_2$  compact layer was deposited on the fluorine-doped tin oxide (FTO, Solaronix, TCO22-7) by dipping the substrate into  $TiCl_4$  followed by an annealing at 450 °C for 30 min. A mesoporous  $TiO_2$  was subsequently deposited from precursor paste (Solaronix, Ti-Nanoxide HT) by doctor blading. The electrodes were sequentially annealed at 75 °C for 10 min, 135 °C for 10 min, 175 °C for 20 min, 425 °C for 10 min, and 450 °C for 10 min. The  $TiO_2$  electrode thus prepared was treated with oxalic acid (0.05 M in ethanol solution) for 1 h, washed in ethanol thoroughly, and finally dried in an  $N_2$  flush. Hereafter untreated  $TiO_2$  and oxalic acid treated  $TiO_2$  are termed WO- $TiO_2$  and OA- $TiO_2$  electrodes, respectively. For dye sensitization, both WO- $TiO_2$  and OA- $TiO_2$  electrodes were dipped in N719 dye solution (0.3 mg/mL in ethanol) for 24 h. These electrodes are termed N719\_WO- $TiO_2$  and N719\_OA- $TiO_2$ , respectively. The DSSC (area  $\sim 0.1$  cm<sup>2</sup>) was assembled by clipping together a photoelectrode and Pt electrode having a 20  $\mu$ m spacer. A solution of 0.1 M LiI and 0.05 M  $I_2$  in dry acetonitrile was used as an electrolyte.

**2.2. Characterization of the Oxalic Acid Treated Electrode.** The current–voltage ( $J$ – $V$ ) characteristics of the cells were recorded on a potentiostat/galvanostat (PGSTAT 30, Autolab Eco Chemie, Utrecht, The Netherlands) under the irradiation of 100 mW/cm<sup>2</sup> at AM 1.5 G using a solar simulator (Sciencetech, London, Ontario, Canada). Prior to the measurements, the intensity of the solar simulator was calibrated using a reference silicon solar cell. To estimate dye loading, the UV/vis spectroscopy was carried out using a double-beam UV-vis spectrophotometer (Jasco, V 530), and all spectra were baseline corrected for quantitative analysis. The extent of dye loading was estimated by desorbing a dye-sensitized electrode (area  $\sim 1$  cm<sup>2</sup>) from 0.1 M aqueous KOH (2 mL) solution and then recording the absorbance spectrum. The binding modes of oxalic acid on the  $TiO_2$  surface as well as dye molecules after treating the  $TiO_2$  surface with oxalic acid were deduced from FTIR spectroscopy using a Bruker spectrometer (Vertex 80 V) at a resolution of 4 cm<sup>-1</sup>. To investigate further the anchoring mode of the N719 dye molecules to the oxalic acid treated  $TiO_2$  surface, XPS was carried out using Mg K $\alpha$  source (Riber MBE system). The binding energy scale was calibrated to the Au 4f<sub>7/2</sub> line of 83.95 eV. Because the actual binding mode of

ruthenium complexes is often hindered due to the overlapping absorptions in the 1400–1600 cm<sup>-1</sup> range, we confirmed the results by using EXAFS, which is a useful technique for probing the co-ordination changes occurring around the element of interest. EXAFS experiments were carried out at Deutsches Elektronen Synchrotron (DESY), Hamburg, Germany, at the P06 beamline in transmission mode. The energy calibrations were carried out using the characteristics Ru k-edge at 22 127 eV of ruthenium.

## 3. RESULTS AND DISCUSSION

Figure 2 shows typical photovoltaic characteristics of the DSSCs fabricated using N719\_OA- $TiO_2$  and N719\_WO- $TiO_2$

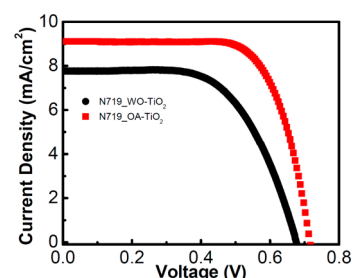


**Figure 2.**  $J$ – $V$  measurements of the DSSCs based on untreated and carboxylic acid treated  $TiO_2$  electrode sensitized with N719 dye, under AM 1.5 G intensity 100 mW/cm<sup>2</sup>.

photoanodes under illumination of AM 1.5 G (intensity, 100 mW/cm<sup>2</sup>). As shown in the figure, the photovoltaic parameters of the devices fabricated using N719\_OA- $TiO_2$  are superior to those fabricated using N719\_WO- $TiO_2$  electrodes. The overall efficiency of 4.6% ( $\pm 0.1$ ) is obtained for the device using N719\_OA- $TiO_2$  photoanodes as compared to 3.2% ( $\pm 0.16$ ) device efficiency using N719\_WO- $TiO_2$  electrodes. The detailed analyses of various photovoltaic parameters of devices are presented in our earlier paper.<sup>17</sup> It has been demonstrated that OA-treatment of  $TiO_2$  leads to the following beneficial effects: (i) improvement in  $V_{OC}$  due to the CBE and quasi Fermi level shift as well as reduced recombination and (ii) increase in the amount of dye loading, e.g., the amount of N719 dye loaded onto OA- $TiO_2$  was  $3.2 \times 10^{-5}$  mol/cm<sup>2</sup>, which is significantly higher than that onto  $TiO_2$  electrodes ( $2.3 \times 10^{-5}$  mol/cm<sup>2</sup>). In this paper, we focus on the investigation of the binding mechanism of N719 dye onto oxalic acid treated  $TiO_2$  electrodes using various techniques discussed below.

**3.1. UV-Vis Spectroscopy.** The UV-vis spectra of dye loaded on WO- $TiO_2$  and OA- $TiO_2$  were recorded taking  $TiO_2$  as reference electrode, and the results are presented in Figure 3a. As shown in the figure, the N719 dye exhibits peaks at 399 and 540 nm, corresponding to metal-to-ligand charge transfer (MLCT) transitions. It may be noted that the higher-energy MLCT has some character of  $\pi$ – $\pi^*$  (ligand centered) transition. Major inferences drawn from this figure are as follows:

- The absorbance of the dye loaded onto OA- $TiO_2$  is higher than that onto WO- $TiO_2$  electrodes, which corroborates our earlier results that higher N719 dye loading takes place onto OA- $TiO_2$  electrodes.
- The low-energy MLCT band reveals a blue shift from 540 to 525 nm for N719 dye loaded onto OA- $TiO_2$  electrodes. The blue shift may be attributed to an increase in the energy of the LUMO of the ligand,



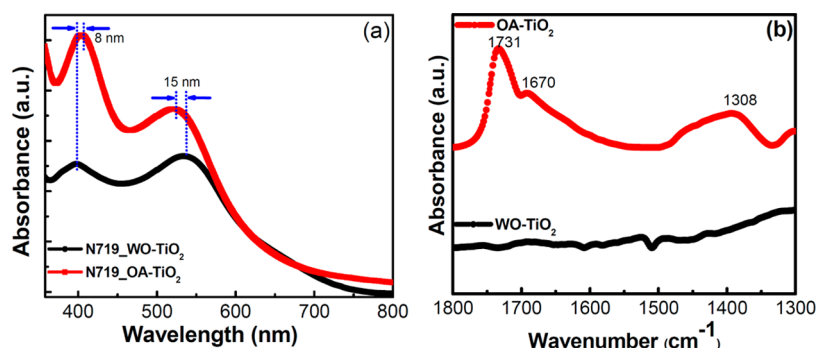


Figure 3. (a) UV-vis spectra of N719 dye-loaded  $\text{TiO}_2$  and OA- $\text{TiO}_2$  surfaces and (b) FTIR spectra of WO- $\text{TiO}_2$  and OA- $\text{TiO}_2$  surfaces.

causing  $\pi-\pi^*$  transitions to occur at higher energies. Because the shape of the absorbance curve has not changed, we rule out dye aggregation as the cause of this shift. Therefore, this blue shift might arise because of an interaction between N719 dye and the oxalate ions present on the  $\text{TiO}_2$  surface.

- (iii) There is a slight red shift in the higher-energy MLCT band from 399 to 407 nm for N719\_OA- $\text{TiO}_2$ . This is expected to have resulted from the increased delocalization of  $\pi$ -electrons in the system for N719\_OA- $\text{TiO}_2$  electrodes. This suggests that the anchoring of the N719 dye to OA- $\text{TiO}_2$  is different from the anchoring of the dye on the WO- $\text{TiO}_2$  electrode. To understand the effect of the type of dye anchoring on device efficiency, we examined the anchoring mechanism of the dyes on the OA- $\text{TiO}_2$  electrodes using various spectroscopic techniques as discussed below.

### 3.2. Fourier Transform Infrared (FTIR) Spectroscopy.

Before analyzing how the dye is anchored onto OA- $\text{TiO}_2$  electrodes, we first investigated the changes that occurred to the  $\text{TiO}_2$  surface when subjected to oxalic acid treatment. For this purpose, we recorded the FTIR spectra of OA- $\text{TiO}_2$  as well as that of  $\text{TiO}_2$  electrodes, and the results are shown in Figure 3b. The FTIR spectra of oxalic acid absorbed on  $\text{TiO}_2$  shows two bands at 1731 and 1697  $\text{cm}^{-1}$ , which are due to splitting of two similar carbonyl ( $\text{C}=\text{O}$ ) groups.<sup>18</sup> These bands are assigned to either bidentate chelating or bidentate bridging ring structure with one oxygen of each carboxylic group coordinated to the surface sites and two  $\text{C}=\text{O}$  double bonds pointing away from the surface. DFT calculation and ATR-FTIR spectroscopic results by Mendive et al. propose the existence of both types of binding modes at the  $\text{TiO}_2$  surface.<sup>19</sup> The increase in loading of N719 dye OA- $\text{TiO}_2$  electrode as discussed earlier may be attributed to the bridging mode of oxalic acid on the  $\text{TiO}_2$  surface. Furthermore, we recorded the FTIR spectra for dye loaded onto WO- $\text{TiO}_2$  as well as OA- $\text{TiO}_2$  electrode and normalized the spectra using intensity of the bipyridine ( $\text{C}=\text{C}$ ) at 1542  $\text{cm}^{-1}$  as an internal standard (Figure 4a,b). The peak assignments are summarized in Table 1.

The IR spectra of the free dye show the presence of carboxylic acid and carboxylate groups as evident by the  $\nu_{\text{C}=\text{O}}$ ,  $\nu_{\text{C}-\text{O}}$ , and  $\nu_{\text{COO}^-}$ ,<sub>asym</sub> and  $\nu_{\text{COO}^-}$ ,<sub>sym</sub> vibrational modes.<sup>10</sup> In the case of dye loaded on WO- $\text{TiO}_2$ , the asymmetric and symmetric stretching modes of  $\text{COO}^-$  are observed at 1615 and 1373  $\text{cm}^{-1}$ , respectively.<sup>10</sup> On the other hand, these bands are shifted to slightly higher binding energy ( $\sim 6$   $\text{cm}^{-1}$ ) in the case of N719 dye loaded onto the OA- $\text{TiO}_2$  surface. This suggests that interaction of N719 dye molecules on the OA-

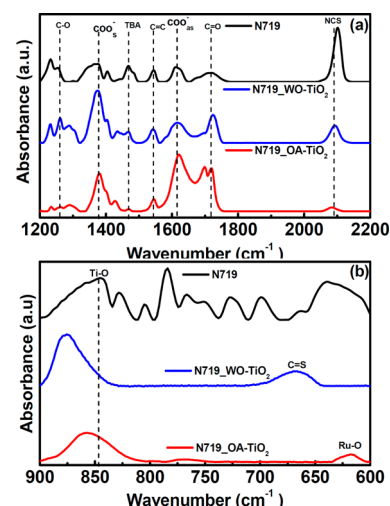


Figure 4. FTIR spectra of free N719 dye as well as N719 dye loaded onto WO- $\text{TiO}_2$  and OA- $\text{TiO}_2$  surfaces in the (a) 1200–2200  $\text{cm}^{-1}$  and (b) 600–900  $\text{cm}^{-1}$  frequency ranges.

Table 1. Peak Assignments of the FTIR Spectra of the N719 Dye-Sensitized WO- $\text{TiO}_2$  and OA- $\text{TiO}_2$  electrode

mode of vibration	$\nu$ ( $\text{cm}^{-1}$ ) N719 dye	$\nu$ ( $\text{cm}^{-1}$ ) N719_WO- $\text{TiO}_2$	$\nu$ ( $\text{cm}^{-1}$ ) N719_OA- $\text{TiO}_2$
bulk $\text{TiO}_2$	-	554	565
$\text{C}=\text{S}$	836	832	absent
$\text{Ru}-\text{O}$	absent	absent	864
$\text{C}-\text{O}$	1256	1261	1261
Sym ( $\text{COO}^-$ )	1372	1373	1379
Bpy	1400	1403	1401
TBA	1464	1468	1471
$\text{C}=\text{C}$	1542	1542	1542
Asym ( $\text{COO}^-$ )	1624	1615	1621
$\text{C}=\text{O}$ (oxalic acid)	absent	absent	1698
$\text{C}=\text{O}$ (dye)	1710	1723	1719
NCS	2102	2095	2085

$\text{TiO}_2$  surface is different than that on the WO- $\text{TiO}_2$  surface. In addition to these peaks, two bands at 1698 and 1719  $\text{cm}^{-1}$  are also observed in the N719 dye loaded onto OA- $\text{TiO}_2$  electrode; these bands arise because of the carbonyl group of oxalic acid as well as that of the dye. The relative intensity of the band at 1719  $\text{cm}^{-1}$  with respect to that at 1698  $\text{cm}^{-1}$  is decreased, implying the involvement of oxalate ions present at the  $\text{TiO}_2$  surface in the binding of N719 dye. Furthermore, the occurrence of TBA peaks in the case of dye loaded onto

WO-TiO<sub>2</sub> and OA-TiO<sub>2</sub> rules out the possibility of anchoring of the dye through covalent bonding of carboxylate groups. It was suggested by Hirose et al. that in order to dissociate TBA from the N719 molecule, it must react with the Ti–OH/TiOH<sub>2</sub> groups.<sup>20,21</sup> The difference ( $\Delta\nu$ ) between  $\nu_{\text{COO}^-}$ ,<sub>asym</sub> and  $\nu_{\text{COO}^-}$ ,<sub>sym</sub> vibrational modes has been related to the type of co-ordination mode of carboxylate group to metal ions by an empirical rule derived by Deacon and Phillips.<sup>22</sup> In particular, the solid state ( $\Delta\nu_{\text{salt}}$ ) and the absorbed state ( $\Delta\nu_{\text{ads}}$ ) have been used to determine bond coordination in carboxylate and carboxylic acid groups. Accordingly, the nature of binding mode can be inferred from the following criterion: if  $\Delta\nu_{\text{ads}} > \Delta\nu_{\text{salt}}$ , the bonding is unidentate, but if  $\Delta\nu_{\text{ads}} < \Delta\nu_{\text{salt}}$ , the chelate or bridge mode occurs. Under the condition  $\Delta\nu_{\text{ads}} \ll \Delta\nu_{\text{salt}}$ , the chelating is the binding mode. The  $\Delta\nu$  value for free dye and the dye absorbed onto WO-TiO<sub>2</sub>/OA-TiO<sub>2</sub> is 252 and 242 cm<sup>-1</sup>, respectively, suggesting bidentate chelating or bridging bonding. It may be noted here that this mode could arise because of bidentate chelating or bridging bonding of COO<sup>-</sup> group of oxalate ions present at the TiO<sub>2</sub> surface in the case of dye loaded on OA-TiO<sub>2</sub> electrode.

To further clarify the binding mechanism, we have focused on the region 1200–2200 cm<sup>-1</sup> (Figure 4a), where peaks corresponding to C=O, COO<sup>-</sup>, and NCS appear. The major observations from this region are:

- The peak corresponding to C=O is present in the case of free dye as well as N719 dye on WO- and OA-TiO<sub>2</sub> electrodes, suggesting that some of the absorbed dye is not bound to the TiO<sub>2</sub> surface via bidentate chelating or bridging bonding mode and some additional binding modes of N719 dye to the WO- and OA-TiO<sub>2</sub> electrodes may be present.
- The peak corresponding to the NCS group is shifted toward a lower wavenumber (from 2102 to 2095 cm<sup>-1</sup>) when the dye is absorbed onto the WO-TiO<sub>2</sub> surface. Though such observations were also made by previous studies, the role of NCS in binding of the N719 dye to TiO<sub>2</sub> electrode was not elaborated much. It was suggested by Johansson et al.<sup>14</sup> as well as Lee et al.<sup>15</sup> that N719 dye may also bind to the TiO<sub>2</sub> surface through the NCS group. The striking features of the dye absorbed onto the OA-TiO<sub>2</sub> electrode are (a) a large shift of ~10 cm<sup>-1</sup> for the peak corresponding to NCS group toward lower wavenumbers and (b) significant reduction in intensity of this peak.

These observations suggest that an NCS group plays a significant role in the anchoring of N719 dye to the OA-TiO<sub>2</sub> surface. This is also confirmed by the disappearance of the 843 cm<sup>-1</sup> peak corresponding to C=S groups in the case of N719 dye-sensitized OA-TiO<sub>2</sub> electrode (Figure 4b). The peak at 832 cm<sup>-1</sup> is assigned to C=S of NCS group of the N719 dye absorbed onto WO-TiO<sub>2</sub> electrode. However, this peak is missing and instead an intense peak is observed at 864 cm<sup>-1</sup> in the case of N719 dye-sensitized on OA-TiO<sub>2</sub> electrode. This peak cannot be assigned to the C=S stretching mode. The reason is that the intensity of the peak corresponding to NCS in the N719\_OA-TiO<sub>2</sub> electrode is much less than that in the N719\_WO-TiO<sub>2</sub> electrode; therefore, we should have observed a very weak peak, if any, corresponding to the C=S bond. This peak is assigned to Ru–O, which might have resulted from the interaction of the N719 dye with oxalate ions present at the OA-TiO<sub>2</sub> surface.<sup>23</sup>

Furthermore, the relative amount of bound N719 dye molecules on the TiO<sub>2</sub> surface has been estimated by the relative intensity of the peak at free carboxylic acid (C=O, 1723 cm<sup>-1</sup>) and carboxylate groups (COO<sup>-</sup>, 1373 cm<sup>-1</sup>).<sup>24,25</sup> Because the carbonyl group peak at 1719 cm<sup>-1</sup> for the OA-TiO<sub>2</sub> electrode has contributions from the dye as well as oxalic acid, it is difficult to determine quantitatively the amount of N719 dye on the OA-TiO<sub>2</sub> surface. Nevertheless, the decrease in the intensity of this peak may be related to the increased amount of dye loading on the OA-TiO<sub>2</sub> surface as compared with the WO-TiO<sub>2</sub> surface. This corroborates our results of a higher amount of N719 dye loading on the OA-TiO<sub>2</sub> surface as compared with the WO-TiO<sub>2</sub> surface. The presence of more N719 dye molecules on the OA-TiO<sub>2</sub> electrode then resulted in enhanced light harvesting and additional photoinduced electrons in the DSSC as compared with the results of WO-TiO<sub>2</sub> electrodes.<sup>26</sup>

**3.3. X-ray Photoelectron Spectroscopy.** To further confirm our findings of FTIR spectra, we have recorded XPS spectra of N719 dye loaded on WO-TiO<sub>2</sub> and OA-TiO<sub>2</sub>. XPS is a highly surface sensitive technique to distinguish between different chemical states of the same atom. The obtained findings are discussed below.

**Ti 2p.** As shown in Figure 5, the splitting due to spin–orbit coupling is observed in the case of dye sensitized on the WO-

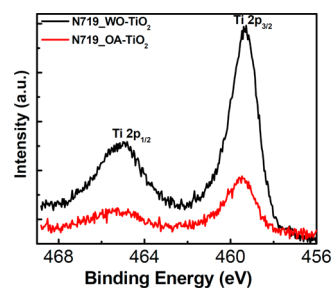


**Figure 5.** XPS spectra of Ti 2p states for N719 dye-sensitized TiO<sub>2</sub> and OA-TiO<sub>2</sub> electrodes.

TiO<sub>2</sub> and OA-TiO<sub>2</sub> electrodes. These Ti 2p peaks at 459.3 eV and 465.1 eV can be attributed to Ti<sup>4+</sup> 2p<sub>3/2</sub> and Ti<sup>4+</sup> 2p<sub>1/2</sub> states, respectively. This suggests that the surface of TiO<sub>2</sub> electrodes comprises only titanium(IV) dioxide and suboxides, i.e., TiO, Ti<sub>2</sub>O<sub>3</sub>, etc. are not present.<sup>15</sup> In the case of dye-sensitized on OA-TiO<sub>2</sub>, these Ti 2p peaks are shifted to binding energies that are slightly higher than those of WO-TiO<sub>2</sub>. The shift to higher binding energies could be due to a change in the surface dipole and/or a change in the Fermi level position in the band gap as a result of oxalic acid treatment of TiO<sub>2</sub> surface. Such changes were also reflected in the UV–vis spectrum, where a blue shift of 15 nm is observed for dye-sensitized OA-TiO<sub>2</sub> electrodes. In addition to the shift in binding energy, a decrease in intensity of Ti 2p peaks is also observed, indicating absorption of oxalate ions on the TiO<sub>2</sub> surface.

**C 1s.** The C 1s spectra of dye-sensitized WO-TiO<sub>2</sub> and OA-TiO<sub>2</sub> are shown in Figure 6a,b. The spectra reveal four peaks upon deconvolution having full width half-maximum (FWHM) of 1.48 and 1.46 eV for N719\_WO-TiO<sub>2</sub> and N719\_OA-TiO<sub>2</sub>, respectively. It is to be noted here that the Ru 3d<sub>3/2</sub> peak is hidden under the major C 1s peak (285.9 eV).<sup>27</sup> The XPS studies of pyridine and pyridine–carboxylic acid adsorbed on TiO<sub>2</sub> surface showed that the C 1s peak due to the pyridine ring and carboxylic group occurs at 284 and 289 eV,

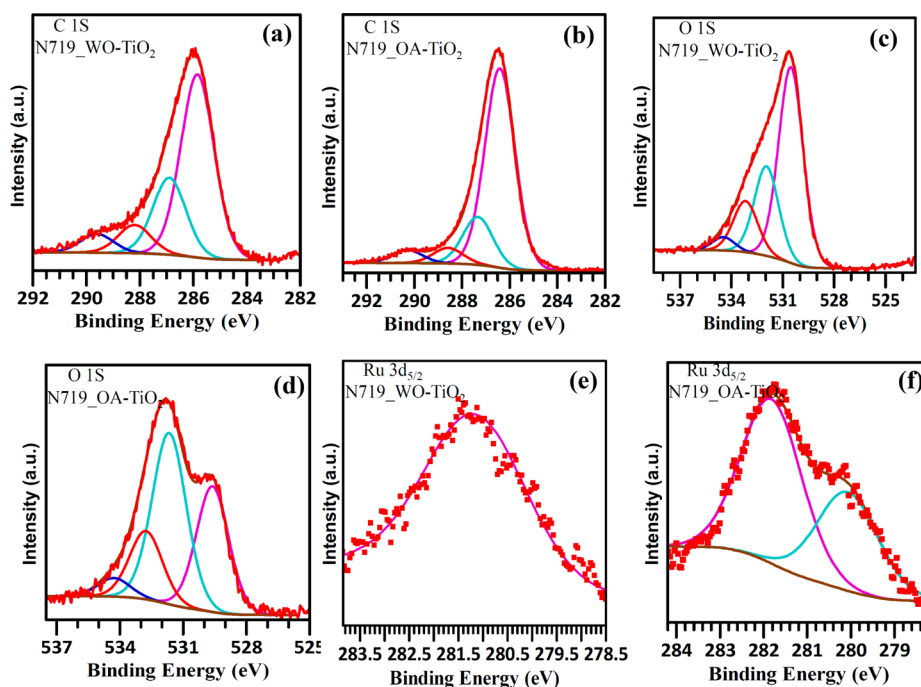


**Figure 6.** XPS spectra of (a, b) C 1s, (c, d) O 1s, and (e, f) Ru 3d<sub>5/2</sub> states for N719 dye-sensitized WO-TiO<sub>2</sub> and OA-TiO<sub>2</sub> electrodes.

respectively.<sup>28</sup> However, in the case of dye-sensitized TiO<sub>2</sub>, the main C 1s peak contains contributions from TBA and NCS groups as well. Therefore, the main C 1s peak at 285.9 eV is contributed by C=C, C-C, C-O, C=N, TBA, and Ru 3d<sub>5/2</sub>. The smaller peaks at 288.3 and 289.6 eV are attributed to O=C=O/C=O from COOH/COO<sup>-</sup> groups and adsorbed CO<sub>2</sub>, respectively.<sup>29</sup> The contributions from the adsorbed organic contaminants in the sample is associated with the peak at 286.9 eV.<sup>30</sup> C 1s XPS spectrum for dye-sensitized OA-TiO<sub>2</sub> electrodes upon deconvolution shows peaks similar to that of WO-TiO<sub>2</sub> electrodes loaded with N719 dye. However, a small shift in peak positions to higher binding energy is observed, indicating that the chemical environment of the C is changed when TiO<sub>2</sub> is treated with oxalic acid.

**O 1s.** The O 1s spectra can provide information about the bonding interaction and surface geometrical structure of the anchoring group. The O 1s XPS spectra of dye-sensitized WO-TiO<sub>2</sub> and OA-TiO<sub>2</sub> both exhibit asymmetrical broadening toward the higher binding energy side, as shown in Figure 6c,d. The deconvolution of the dye-sensitized TiO<sub>2</sub> shows four well-resolved peaks; FWHM for all the fitted peaks of N719\_WO-TiO<sub>2</sub> and N719\_OA-TiO<sub>2</sub> are 1.67 and 1.65 eV, respectively. The peaks at 530.5 and 531.9 eV are attributable to O<sup>-</sup> and Ti-OH from the TiO<sub>2</sub> surface, respectively. The peak at 531.9 eV also has some contribution from a C=O group of the dye. The peak at 533.2 eV is assigned to COOH groups of the dye as well as Ti-OH<sub>2</sub>. In addition, the peak at 534.5 eV can be attributed to the adsorbed organic contaminants. The observed deconvoluted peaks are in accordance with those reported in the literature.<sup>15</sup> When the N719 dye is loaded onto the WO-TiO<sub>2</sub> electrode, the peak corresponding to COOH and C=O groups of the dye are shifted to the lower binding energy side. This suggests that the chemical environment around O is different from that of the dye-loaded WO-TiO<sub>2</sub> electrode. The main feature of the O 1s XPS spectrum of N719 sensitized on OA-TiO<sub>2</sub> is the appearance of a new well-resolved peak at 529.5 eV and the disappearance of the peak corresponding to the O<sup>-</sup>

at the WO-TiO<sub>2</sub> surface. The new peak at 529.5 eV is assigned to a Ru-O bond.<sup>31,32</sup> The origin of this new peak may be due to the substitution of an NCS group of the dye by O<sup>-</sup> of the oxalic acid. In addition, the disappearance of the O<sup>-</sup> peak could be due to large electron scattering arising from the presence of oxalate ions and the dye layer on the WO-TiO<sub>2</sub> surface.

**Ru 3d<sub>5/2</sub>.** The splitting due to spin-orbit coupling is observed corresponding to the Ru of the dye, i.e., Ru 3d<sub>3/2</sub> and Ru 3d<sub>5/2</sub>. The Ru 3d<sub>3/2</sub> peak overlaps with the C 1s peak, and therefore, it is difficult to extract information by deconvolution of this peak. However, the Ru 3d<sub>5/2</sub> peak reveals a shift of 4.2 eV from the Ru 3d<sub>3/2</sub> peak.<sup>27</sup> Therefore, the Ru 3d<sub>5/2</sub> peak can be utilized to extract further information about the chemical state of Ru. Figure 6e,f shows the XPS spectrum of Ru 3d<sub>5/2</sub> for N719 dye-sensitized onto TiO<sub>2</sub> and OA-TiO<sub>2</sub>. In the case of Ru, FWHM for all the fitted peaks of N719\_WO-TiO<sub>2</sub> and N719\_OA-TiO<sub>2</sub> are 1.63 and 1.64 eV, respectively. As shown in Figure 6e, the peak at 281.3 eV is attributed to Ru 3d<sub>5/2</sub> arising because of the adsorbed N719 dye molecules on the WO-TiO<sub>2</sub> surface.<sup>15</sup> In the case of N719 loaded onto OA-TiO<sub>2</sub>, the Ru 3d<sub>5/2</sub> is deconvoluted into two peaks: the peak at 281.9 eV is attributable to the dye molecules absorbed on TiO<sub>2</sub> surface as in the case of the N719\_WO-TiO<sub>2</sub> surface, while a well-resolved peak at 280.1 eV is assigned to the Ru-O bond. This Ru-O bond occurs because of a chemical bond between dye molecules and oxalate ions present at the OA-TiO<sub>2</sub> surface. This is in line with our earlier observation of FTIR data in which the signature of the Ru-O bond is observed in dye loaded onto the OA-TiO<sub>2</sub> electrode.

**S 2p.** The S 2p spectra of N719 dye loaded onto WO-TiO<sub>2</sub> show contributions from the sulfur of NCS groups due to spin-orbit coupling. This is similar to the reports by other researchers of two peaks that are observed and assigned to the contributions arising from the interaction between an NCS ligand and the dye. More strikingly, these peaks are not observed in the case of N719 dye-sensitized onto OA-TiO<sub>2</sub>, as shown in Figure 7. This confirms our earlier assumption based



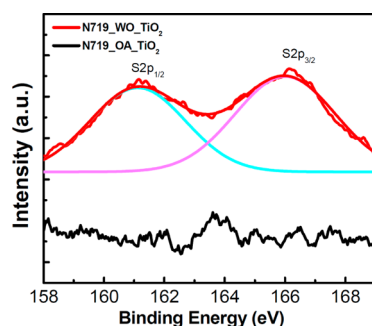


**Figure 7.** XPS spectra of S 2p states for N719 dye-sensitized WO-TiO<sub>2</sub> and OA-TiO<sub>2</sub> electrode.

on FTIR data and O 1s XPS data that an NCS group of the N719 dye is substituted by the O<sup>−</sup> group of oxalate ions present at the OA-TiO<sub>2</sub> surface.

### 3.4. Extended X-ray Absorption Fine Structure.

Because the NCS ligand is the weakest one in the dye molecule, it is likely to be replaced more easily than the other carboxylate or carboxylic acid group ligand upon absorption onto the TiO<sub>2</sub> surface, as was suggested by our FTIR and XPS data. To confirm this, we have focused on the Ru atom and its surroundings and recorded EXAFS spectra in the spectral region extending from 100 eV below to 1000 eV above a core level excitation k-edge of ruthenium. After the atomic background absorption subtraction, the EXAFS ( $\chi$ ) was extracted from the measured data. For a quantitative comparison of the local structural properties, the data was Fourier transformed to R-space to obtain radial distribution function. A set of EXAFS data analysis program available within the IFEFFIT software package has been used for fitting of experimental data using the following equation:

$$\chi = \sum_j \frac{N f_j(k) \exp[-2k^2 \sigma_j^2] \exp\left[\frac{-2R_j}{\lambda}\right]}{k R_j^2} \sin[2kR_j + \delta_j(k)]$$

where  $f(k)$  is the amplitude function for  $j$ th shell,  $\delta(k)$  the phase shift,  $\lambda$  the electron mean free path, and  $N_j$  the number of neighboring atoms in the  $j$ th shell at a distance  $R_j$  from the central atom. For the fitting of the data, bond distance ( $R$ ), coordination number ( $N$ ), and disorder (Debye–Waller) factor ( $\sigma^2$ ) were used as variable parameters. As shown in Figure 1a, N719 dye has a complex structure having two nitrogen atoms bonded to NCS groups and four nitrogen bonded to the bipyridine ligand. Owing to the complex structure, we have fitted only the first two peaks of the EXAFS spectra. In the case of N719\_WO-TiO<sub>2</sub>, these peaks correspond to the first two coordination shells having two and four nitrogen atoms, respectively, (Figure 8a). The parameters derived from fitting results are summarized in Table 2. As shown in the table, the bond lengths for Ru and nitrogen are 2.052 and 2.108 Å, respectively, for nitrogen bonded at NCS group and bipyridine, respectively. These bond lengths values are similar to those reported in the literature for free N719 dye.<sup>33</sup> A slight deviation of the bond lengths could arise because of the chemical bonding of N719 to the WO-TiO<sub>2</sub> surface.

However, for N719\_OA-TiO<sub>2</sub>, reasonable fitting could not be established under these assumptions, i.e., considering only the first two co-ordination shells of nitrogen atoms. When Ru–O bonding, as revealed from our XPS and FTIR data, was taken into account, the best fit was obtained (Figure 8b). Therefore,

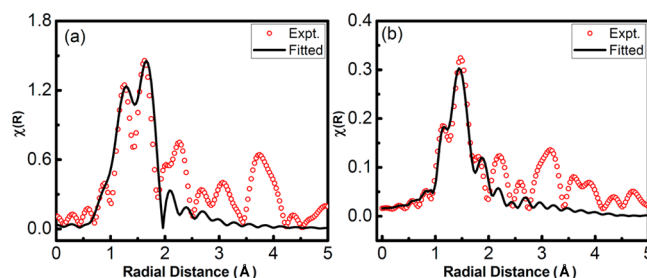


**Figure 8.** Fourier transforms of the EXAFS function  $\kappa^3\chi(\kappa)$  for (a) untreated and (b) carboxylic acid treated dye-sensitized TiO<sub>2</sub> samples.

**Table 2. Local Structural Parameters of the N719 Dye-Sensitized WO-TiO<sub>2</sub> and OA-TiO<sub>2</sub> Electrode as Derived from Fitted EXAFS Spectra**

photoelectrode (coordination shell)	parameter	N719_WO-TiO <sub>2</sub>	N719_OA-TiO <sub>2</sub>
Ru–N(1)	$N$ (atoms)	2	1
	$R$ (Å)	$2.052 \pm 0.03$	$2.057 \pm 0.04$
	$\sigma^2$ (Å <sup>2</sup> )	0.005	0.005
Ru–N(2)	$N$ (atoms)	4	4
	$R$ (Å)	$2.108 \pm 0.02$	$2.125 \pm 0.05$
	$\sigma^2$ (Å <sup>2</sup> )	0.003	0.006
Ru–O(1)	$N$ (atoms)	–	1
	$R$ (Å)	–	$1.657 \pm 0.06$
	$\sigma^2$ (Å <sup>2</sup> )	–	0.003

in this case, three co-ordination shells were considered during fitting; the first co-ordination shell has one oxygen atom, the second one nitrogen atom, and the third 4 nitrogen atoms. The Ru–N bond length deduced from the fitting curves are 2.057 and 2.125 Å, corresponding to nitrogen at the NCS group and bipyridine, respectively. These values are almost the same as those in the case of N719\_WO-TiO<sub>2</sub>. In addition, the Ru–O bond length, as estimated from the fitting, is 1.657 Å, which is in agreement with the values reported in the literature.<sup>34</sup>

**3.5. Proposed Binding Scheme and Implication of Dye Binding on Photovoltaic Properties.** On the basis of all spectroscopic and EXAFS data, we propose the binding of N719 dye on WO-TiO<sub>2</sub> and OA-TiO<sub>2</sub> surfaces. In the proposed model, N719 dye molecules adsorb on the WO-TiO<sub>2</sub> surface via the COOH groups as well as through some interaction via an NCS group, as shown in Figure 1f. However, the anchoring of the N719 dye via carboxylate/carboxylic acid groups is ruled out at the OA-TiO<sub>2</sub> surface. Since NCS is the weakest ligand in the N719 dye, the possibility of binding the N719 dye to the OA-TiO<sub>2</sub> surface through this group is greater than that via the carboxylate/carboxylic acid groups. This was complemented by our FTIR data, where a peak corresponding to NCS diminishes significantly. The same is also confirmed by EXAFS data, where a better fit is observed, corresponding to a Ru–O bond and not a Ru–NCS bond. Therefore, on the basis of these results, it is suggested that the N719 dye binds to the OA-TiO<sub>2</sub> surface through interaction between the Ru atom of the dye and O<sup>−</sup> present at the OA-TiO<sub>2</sub> surface due to oxalate ions, as shown schematically in Figure 9.

The role of oxalic acid treatment of TiO<sub>2</sub> surface can be summarized as follows:



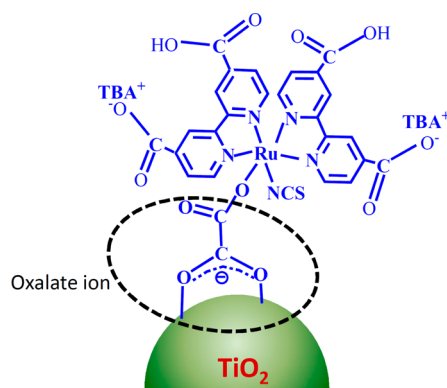


**Figure 9.** Schematic presentation of binding of N719 dye on oxalic acid treated  $\text{TiO}_2$  surface.

- (i) The binding of the N719 via carboxylate ions present at the OA- $\text{TiO}_2$  surface may allow more effective transfer of electrons because of increased conjugation as compared to untreated  $\text{TiO}_2$  surface.<sup>35</sup>
- (ii) Being a strong acid ( $\text{pK}_a$  1.23), the oxalic acid chelates to Ti atoms on the  $\text{TiO}_2$  surface via strong bridging binding and allows more dye loading onto the OA- $\text{TiO}_2$  electrode as described earlier.
- (iii) In addition to providing assistance for more dye loading, the oxalic acid occupied sites also act as a passivation layer. This was confirmed in our earlier observations of impedance spectroscopy measurements, where an increased recombination lifetime is observed for OA- $\text{TiO}_2$ -based DSSCs.<sup>36</sup>

#### 4. CONCLUSION

In summary, we have studied the binding behavior of the N719 dye through detailed spectroscopic investigation, namely, FTIR, UV-vis, and XPS spectroscopy and EXAFS measurements. The UV-vis spectra imply a strong interaction between the dye and the oxalic acid, which assists more dye loading onto the OA- $\text{TiO}_2$  surface. The FTIR and XPS spectroscopy revealed that binding of N719 dye onto the OA- $\text{TiO}_2$  surface is different from that onto the WO- $\text{TiO}_2$  electrode. The N719 dye binds to the OA- $\text{TiO}_2$  surface through interaction between the Ru atom of the dye and  $\text{O}^-$  present at the OA- $\text{TiO}_2$  surface due to oxalate ions. On the other hand, the binding of the dye to untreated  $\text{TiO}_2$  surface occurs through carboxylic acid group. The results were confirmed by EXAFS measurements, which also show reasonable fitting for Ru-O bond in the case of N719\_OA- $\text{TiO}_2$  electrodes. The different binding mechanism of the N719 dye on the oxalic acid treated  $\text{TiO}_2$  electrode resulted in improved photovoltaic characteristics of DSSCs based on N719 dye-sensitized OA- $\text{TiO}_2$  electrodes.

#### AUTHOR INFORMATION

##### Corresponding Authors

\*E-mail: vibhas@barc.gov.in.

\*E-mail: dkaswal@yahoo.com.

##### Notes

The authors declare no competing financial interest.

#### ACKNOWLEDGMENTS

This work is supported by "DAE-SRC Outstanding Research Investigator Award" (2008/21/05-BRNS) granted to D.K.A.

We are grateful to SINP-DST for providing financial assistance to carry out experiments at DESY, Hamburg, Germany. We are also thankful to Dr. G. Falkenberg, Hamburg, DESY for his kind help during the EXAFS measurements.

#### REFERENCES

- (1) Lee, C.-H.; Hsiao, P.-T.; Lu, M.-D.; Wu, J.-M. Light Harvesting Enhancement for Ti-based Dye-Sensitized Solar Cells by Introducing a Grooved Texture Underlayer. *RSC Adv.* **2013**, *3*, 2216–2218.
- (2) Liu, G.; Li, X.; Wang, H.; Rong, Y.; Ku, Z.; Xu, M.; Liu, L.; Hu, M.; Yang, Y.; Han, H. An Efficient Thiolate/disulfide Redox Couple based Dye-Sensitized Solar Cell with a Graphene Modified Mesoscopic Carbon Counter Electrode. *Carbon* **2013**, *53*, 11–18.
- (3) Manseki, K.; Yu, Y.; Yanagida, S. A Phenyl-Capped Aniline Tetramer for Z907/tert-butylpyridine-based Dye-Sensitized Solar Cells and Molecular Modelling of the Device. *Chem. Commun. (Cambridge, U.K.)* **2013**, *49*, 1416–1418.
- (4) Yang, X.; Yanagida, M.; Han, L. Reliable Evaluation of Dye-Sensitized Solar Cells. *Energy & Environ. Sci.* **2013**, *6*, 54–66.
- (5) Wang, Z.-S.; Yamaguchi, T.; Sugihara, H.; Arakawa, H. Significant Efficiency Improvement of the Black Dye-Sensitized Solar Cell through Protonation of  $\text{TiO}_2$  Films. *Langmuir* **2005**, *21*, 4272–4276.
- (6) Park, K.-H.; Jin, E. M.; Gu, H. B.; Shim, S. E.; Hong, C. K. Effects of  $\text{HNO}_3$  Treatment of  $\text{TiO}_2$  nanoparticles on the Photovoltaic Properties of Dye-Sensitized Solar Sells. *Mater. Lett.* **2009**, *63*, 2208–2211.
- (7) Guai, G. H.; Song, Q. L.; Lu, Z. S.; Ng, C. M.; Li, C. M. Tailor and Functionalize  $\text{TiO}_2$  Compact Layer by Acid Treatment for High Performance Dye-Sensitized Solar Sells and its Enhancement Mechanism. *Renewable Energy* **2013**, *51*, 29–35.
- (8) Hao, S.; Wu, J.; Fan, L.; Huang, Y.; Lin, J.; Wei, Y. The Influence of Acid Treatment of  $\text{TiO}_2$  Porous Film Electrode on Photoelectric Performance of Dye-Sensitized Solar Sells. *Solar Energy* **2004**, *76* (6), 745–750.
- (9) Falaras, P. Synergetic Effect of Carboxylic Acid Functional Groups and Fractal Surface Characteristics for Efficient Dye Sensitization of Titanium Oxide. *Sol. Energy Mater. Sol. Cells* **1998**, *53* (1–2), 163–175.
- (10) Finnie, K. S.; Bartlett, J. R.; Woolfrey, J. L. Vibrational Spectroscopic Study of the Coordination of (2,2'-Bipyridyl-4,4'-dicarboxylic acid)ruthenium(II) Complexes to the Surface of Nanocrystalline Titania. *Langmuir* **1998**, *14*, 2741–2749.
- (11) Nazeeruddin, M. K.; Humphry-Baker, R.; Liska, P.; Grätzel, M. Investigation of Sensitizer Adsorption and the Influence of Protons on Current and Voltage of a Dye-Sensitized Nanocrystalline  $\text{TiO}_2$  Solar Cell. *J. Phys. Chem. B* **2003**, *107*, 8981–8987.
- (12) León, C. P.; Kador, L.; Peng, B.; Thelakkat, M. Characterization of the Adsorption of Ru-bpy Dyes on Mesoporous  $\text{TiO}_2$  Films with UV-Vis, Raman, and FTIR Spectroscopies. *J. Phys. Chem. B* **2006**, *110*, 8723–8730.
- (13) De Angelis, F.; Fantacci, S.; Selloni, A.; Nazeeruddin, M. K.; Grätzel, M. First-Principles Modelling of the Adsorption Geometry and Electronic structure of Ru(II) Dyes on Extended  $\text{TiO}_2$  Substrates for Dye-Sensitized Solar Cell Applications. *J. Phys. Chem. C* **2010**, *114*, 6054–6061.
- (14) Johansson, E. M. J.; Hedlund, M.; Siegbahn, H.; Rensmo, H. Electronic and Molecular Surface Structure of  $\text{Ru}(\text{tcterpy})(\text{NCS})_3$  and  $\text{Ru}(\text{dcby})_2(\text{NCS})_2$  Adsorbed from Solution onto Nanostructured  $\text{TiO}_2$ : A Photoelectron Spectroscopy Study. *J. Phys. Chem. B* **2005**, *109*, 22256–22263.
- (15) Lee, K. E.; Gomez, M. A.; Regier, T.; Hu, Y.; Demopoulos, G. P. Further Understanding of the Electronic Interactions between N719 Sensitizer and Anatase  $\text{TiO}_2$  Films: A Combined X-ray Absorption and X-ray Photoelectron Spectroscopic Study. *J. Phys. Chem. C* **2011**, *115*, 5692–5707.
- (16) Saxena, V.; Veerender, P.; Chauhan, A. K.; Jha, P.; Aswal, D. K.; Gupta, S. K. Efficiency Enhancement in Dye Sensitized Solar Sells

through Co-Sensitization of TiO<sub>2</sub> Nanocrystalline Electrodes. *Appl. Phys. Lett.* **2012**, *100*, 133303.

(17) Saxena, V.; Veerender, P.; Gusain, A.; Jha, P.; Singh, J.; Koiry, S. P.; Varde, P. V.; Chauhan, A. K.; Aswal, D. K.; Gupta, S. K.; Co-Sensitization of N719 and RhCL Dyes on Carboxylic Acid Treated TiO<sub>2</sub> for Enhancement of Light Harvesting and Reduced Recombination. *Org. Electron.*, in press.

(18) Hug, S. J.; Bahnemann, D. Infrared Spectra of Oxalate, Malonate and Succinate Adsorbed on the Aqueous Surface of Rutile, Anatase and Lepidocrocite Measured with in situ ATR-FTIR. *J. Electron Spectrosc. Relat. Phenom.* **2006**, *150* (2–3), 208–219.

(19) Mendive, C. B.; Bredow, T.; Blesa, M. A.; Bahnemann, D. W. ATR-FTIR Measurements and Quantum Chemical Calculations Concerning the Adsorption and Photoreaction of Oxalic Acid on TiO<sub>2</sub>. *Phys. Chem. Chem. Phys.* **2006**, *8*, 3232–3247.

(20) Hirose, F.; Kuribayashi, K.; Suzuki, T.; Narita, Y.; Kimura, Y.; Niwano, M. UV Treatment Effect on TiO<sub>2</sub> Electrodes in Dye-Sensitized Solar Cells with N719 Sensitizer Investigated by Infrared Absorption Spectroscopy. *Electrochem. Solid-State Lett.* **2008**, *11*, A109–A111.

(21) Kuribayashi, K.; Iwata, H.; Hirose, F. N719 Dye Adsorption on Anatase TiO<sub>2</sub> Surfaces Investigated by Infrared Absorption Spectroscopy. *ECS Trans.* **2007**, *6*, 15–19.

(22) Deacon, G. B.; Phillips, R. J. Relationships between the Carbon-Oxygen Stretching Frequencies of Carboxylate Complexes and the Type of Carboxylate Coordination. *Coord. Chem. Rev.* **1980**, *33*, 227–250.

(23) León, C. P. *Vibrational Spectroscopy of Photosensitizer Dyes for Organic Solar Cells*. Cuvillier Verlag: Göttingen, Germany, 2006.

(24) Lim, J.; Kwon, Y. S.; Park, T. Effect of Coadsorbent Properties on the Photovoltaic Performance of Dye-Sensitized Solar Cells. *Chem. Commun.* **2011**, *47*, 4147–4149.

(25) Schiffmann, F.; VandeVondele, J.; Hutter, J. r.; Wirz, R.; Urakawa, A.; Baiker, A. Protonation-Dependent Binding of Ruthenium Bipyridyl Complexes to the Anatase (101) Surface. *J. Phys. Chem. C* **2010**, *114*, 8398–8404.

(26) Kilså, K.; Mayo, E. I.; Brunschwig, B. S.; Gray, H. B.; Lewis, N. S.; Winkler, J. R. Anchoring Group and Auxiliary Ligand Effects on the Binding of Ruthenium Complexes to Nanocrystalline TiO<sub>2</sub> Photoelectrodes. *J. Phys. Chem. B* **2004**, *108*, 15640–15651.

(27) Cai, T.; Song, Z.; Chang, Z.; Liu, G.; Rodriguez, J. A.; Hrbek, J. Ru Nanoclusters Prepared by Ru<sub>3</sub>(CO)<sub>12</sub> Deposition on Au(111). *Surf. Sci.* **2003**, *538*, 76–88.

(28) Schnadt, J.; O'Shea, J. N.; Patthey, L.; Schiessling, J.; Krempaský, J.; Shi, M.; Mårtensson, N.; Brühwiler, P. A. Structural Study of Adsorption of Isonicotinic Acid and Related Molecules on Rutile TiO<sub>2</sub>(110) II: XPS. *Surf. Sci.* **2003**, *544*, 74–86.

(29) Guo, Q.; Cocks, I.; Williams, E. M. The Adsorption of Benzoic Acid on a TiO<sub>2</sub>(110) Surface Studied using STM, ESDIAD and LEED. *Surf. Sci.* **1997**, *393*, 1–11.

(30) Cueto, L.; Hirata, G.; Sánchez, E. Thin-film TiO<sub>2</sub> Electrode Surface Characterization upon CO<sub>2</sub> Reduction Processes. *J. Sol-Gel Sci. Technol.* **2006**, *37*, 105–109.

(31) Kim, K. S.; Winograd, N. X-Ray Photoelectron Spectroscopic Studies of Ruthenium-Oxygen Surfaces. *J. Catal.* **1974**, *35*, 66–72.

(32) Wier, L. M.; Murray, R. W. Chemically Modified Electrodes: VIII. The Interaction of Aqueous with Native and Silanized Electrodes. *J. Electrochem. Soc.* **1979**, *126*, 617–623.

(33) Fantacci, S.; De Angelis, F.; Selloni, A. Absorption Spectrum and Solvatochromism of the [Ru(4,4'-COOH-2,2'-bpy)<sub>2</sub>(NCS)<sub>2</sub>] Molecular Dye by Time Dependent Density Functional Theory. *J. Am. Chem. Soc.* **2003**, *125*, 4381–4387.

(34) Kim, Y. D.; Schwegmann, S.; Seitsonen, A. P.; Over, H. Epitaxial Growth of RuO<sub>2</sub>(100) on Ru(1010): Surface Structure and Other Properties. *J. Phys. Chem. B* **2001**, *105*, 2205–2211.

(35) Hara, K.; Sayama, K.; Ohga, Y.; Shinpo, A.; Suga, S.; Arakawa, H. A Coumarin-Derivative Dye Sensitized Nanocrystalline TiO<sub>2</sub> Solar Cell having a High Solar-Energy Conversion Efficiency up to 5.6%. *Chem. Commun.* **2001**, *6*, 569–570.

(36) Bisquert, J.; Fabregat-Santiago, F.; Mora-Seró, I.; Garcia-Belmonte, G.; Giménez, S. Electron Lifetime in Dye-Sensitized Solar Cells: Theory and Interpretation of Measurements. *J. Phys. Chem. C* **2009**, *113*, 17278–17290.